

Reconstruction using optimal spatially variant kernel for B-mode ultrasound imaging

Hesham Desoky^a, Abou-Bakr M. Youssef^a and Yasser M. Kadah^{a,b1}

^aBiomedical Engineering Department, Cairo University, Egypt

^bEmory University/Georgia Tech Biomedical Engineering, Atlanta 30322

ABSTRACT

We propose a technique that allows the improvement of lateral resolution in ultrasound imaging using a deconvolution-based strategy. We first derive a formulation for the problem in terms of an arbitrary spatially-variant beam pattern and show that it is possible to optimally estimate the values of the image by solving a large linear inverse problem. This linear system depends on the shape and extent of the point spread function as well as the desired resolution of the resultant image. We show that this linear system is sparse and therefore sparse matrix techniques for storage and algebra are used to make the computational cost reasonable. The strategies used to solve this problem are proposed based on truncated singular value decomposition or regularized conjugate gradient method that allows an equivalent regularization to imposing a quadratic inequality constraint. This allows the condition number of the problem to be kept sufficiently low, thus ensuring a robust solution. For a given ultrasound line with specific transmit and receive focusing characteristics, this problem is solved for the whole image and we show that it is possible to implement the solution in a look-up table form similar to what is used in image reconstruction in current ultrasound systems. This accounts for the variations of the point spread function at different spatial positions.

Keywords: Ultrasound imaging, linear systems, deconvolution, spatially-variant point spread function.

1. INTRODUCTION

As all imaging modalities, ultrasound imaging attempts to reconstruct an accurate map of a particular characteristic of the human tissues under practical constraints. Assuming linearity of the image formation process, the quality of image depends mainly on the effective point spread function (PSF) of the imaging system. Therefore, the PSF can be used to describe the way ultrasound images are formed and hence evaluate their spatial resolution characteristics. In ultrasound imaging, resolution is usually described in terms of two parameters; namely axial and lateral resolutions. While the first is mainly a function of the ultrasound transducer and transmitted pulse shape, the second is very much dependent on the spacing of the probe as well as the focusing characteristics of the imaging system. Due to the practical constraints on transducer manufacturing, the lateral resolution is significantly worse than the axial resolution of the system. Moreover, it varies with spatial position inside the field of view, which makes its effect more complicated to interpret and compensate for by sonographers. Therefore, a significant amount of research effort has been directed to account for and remove –or deconvolve– the effect of PSF variations in ultrasound images.

Several strategies have been proposed to address the problem of deconvolution in ultrasound imaging. These strategies include the use of morphological filtration¹, reconstruction filters to account for PSF characteristics for applications where coded excitation during transmission is used^{2,3}, one-dimensional deconvolution using Wiener filtering approach with estimated PSF^{5,6}, homomorphic filtration⁶, higher order statistics (rather than second order statistics)⁷, elevation direction deconvolution for more accurate 3-D imaging⁸, maximum *a posteriori* (MAP) estimation⁹, inverse scattering based on Born approximation¹⁰, lateral beam characteristics only deconvolution¹¹, better estimation of the ultrasound PSF in vivo for more accurate deconvolution¹², blind homomorphic filtering in 2-D and 3-D^{13,14}, and using Bayesian techniques¹⁵. In spite of the wide variety of available techniques and their different approaches to this problem, they share at least one of several limitations that include the assumption of separability of axial and lateral deconvolution

¹ E-mail: ymk@ieee.org

problems, the assumption of spatially-invariant PSF, the lack of optimality in solution, and the extensive amount of computations required to perform the deconvolution task. As a result, the implementation of many of these approaches on practical system has not been addressed. Hence, a new technique that addresses the axial and lateral deconvolution problems simultaneously and allow for spatially-variant point spread function while maintaining a reasonable computational complexity would be rather useful for practical implementation.

In this work, we describe a general linear model for the process of 2-D ultrasound image formation based on a more realistic model of the problem that accounts for both axial and lateral components of the imaging PSF simultaneously. The problem is formulated as a sparse linear system of equations that maps the acquired RF samples directly into the optimal pixel values that represent the desired image. We use sparse matrix tools that allow much smaller computational and storage efforts. The sparse system is then solved using either truncated singular value decomposition or the regularized conjugate gradient iterative technique, which enables a flexible control of the degree of accuracy versus the computation time. It is therefore possible to implement this strategy into current ultrasound imaging systems with reasonable computational effort.

2. THEORY

Consider $f(x,y)$ as the continuous-space spatial domain intensity distribution representing the ideal or optimum resolution ultrasound image. Let the spatially-variant point spread function (PSF) of the system representing the ultrasonic field at point (x_o, y_o) be given as $h(x,y; x_o, y_o)$. Hence, giving the general assumption of system linearity, the acquired points $g(x,y)$ can be computed from the superposition integral as,

$$g(x, y) = \int_{-\infty}^{\infty} \int_{-\infty}^{\infty} f(\alpha, \beta) \cdot h(x, y; \alpha, \beta) d\alpha d\beta \quad (1)$$

Given the method by which the image is usually displayed in practice, the spatial domain can be modeled as piecewise constant function consisting of the sum of shifted gate-like functions representing the pixels of the image up to the desired resolution. That is,

$$f(x, y) = \sum_{n=0}^{N-1} \sum_{m=0}^{M-1} \eta_{n,m} \cdot \Pi(x - x_n, y - y_m) . \quad (2)$$

Consequently, the formula in (1) can be expressed as as,

$$g(x, y) = \int_{-\infty}^{\infty} \int_{-\infty}^{\infty} \sum_{n=0}^{N-1} \sum_{m=0}^{M-1} \eta_{n,m} \cdot \Pi(\alpha - x_n, \beta - y_m) \cdot h(x, y; \alpha, \beta) d\alpha d\beta, \quad (3)$$

which reduces to,

$$g(x, y) = \sum_{n=0}^{N-1} \sum_{m=0}^{M-1} \eta_{n,m} \cdot \hat{h}(x, y; x_n, y_n) . \quad (4)$$

Here, the PSF is replaced by another one that takes into account the resolution of the desired image as evaluated by the integration in (3). Since the data collection has to be performed in a discrete rather than continuous manner, Eq. (4) is evaluated at a finite set of values (x_i, y_i) according to the sampling characteristics. Arranging the acquired samples and desired image intensity values in one-dimensional array form, the problem can be expressed as a linear system of the form,

$$\vec{g} = H \cdot \vec{\eta} . \quad (5)$$

Hence, given the measured values from all transducer elements $g(x_i, y_i)$ and the characteristics of the system and the image resolution as expressed by the matrix H , it is desired to solve the above linear system to obtain the image intensity values $\eta_{n,m}$.

Note that the size of this linear system is very large. For a system that samples data from a N -element probe with a record size of M points per element and a desired image size of $L \times L$, the size of the system matrix H in this linear system is $(N \cdot M) \times (L \cdot L)$, which is problematic using conventional matrix computation tools. However, observing that the PSF of the imaging system has a compact support within the field of view, the system matrix will be sparse. That is, each row has only a few nonzero elements compared to the row size. In fact, it will be in the form of a multi-banded system (i.e.,

nonzero elements lie within several bands of small bandwidth inside the matrix)¹⁸. Therefore, using sparse matrix methods, the solution of the above large linear system can be performed with modest computational/storage requirements that are practical for use in current ultrasound imaging systems. Hence, we propose two strategies that enable this to be done. The first is to use truncated SVD (TSVD) off-line to precompute a reconstruction table (or the inverse operator) for the above problem. The order of such computation is $O(n^3)$, where n is the number of nonzero elements in the system matrix. On the other hand, the second is to use the regularized conjugate gradient method to compute the solution equivalent to TSVD iteratively with low computational burden of $O(n^2)$. This makes the second strategy suitable for real-time computation.

3. METHODS

3.1. Sparse matrix manipulation

Starting from the description of the linear system matrix as a sparse matrix with only very few nonzero elements in each row, the storage of such system can be performed using several techniques. Among the most efficient ways to do that is the row-indexed storage method²¹, which requires only twice the size of the nonzero elements for their storage, which is a very small fraction of the size of the whole matrix. Once this representation is done, matrix-vector multiplication operations are only equal in complexity to the number of nonzero elements. This makes it always computationally feasible even for modest computational platforms. Also, transposition operations are done by reversing the indexing sequence for the matrix, which again is rather simple and does not pose an additional computational burden.

3.2. Conjugate gradient iterative solution

The method of conjugate gradient optimizes the solution of a linear system by removing the error components in a number of directions that span the space of the solution^{18,19}. It has a number of advantages as a result of its unique scheme. The first is that the number of iterations to reach the solution has an upper bound of the dimension of the space of the linear system solution. Moreover, only a few iterations are usually required to reach a good accuracy for the solution. Another advantage is that the solution accuracy can be traded off with computation time rather flexibly. This allows the method to be customized for the particular application at hand by selecting a predetermined value for the number of iterations that correspond to the desired computation time. If accuracy is desired, an efficient implementation of this method may rely on a measure of the solution update in such a way that the stopping criterion is to have an update that is insignificant compared to the present solution. This can be described mathematically in terms of an arbitrary definition of vector norms. Given the sparse matrix format of the system matrix, the computational complexity of each of the conjugate gradient iterations is still in the order of the total number of nonzero elements in the sparse system matrix. This is quite reasonable and can be guaranteed to be equal to or lower than the computational effort of conventional reconstruction techniques. A description of the conjugate gradient iteration used in this work is provided in Appendix I.

Since the deconvolution problem is notorious for being ill-posed, it is necessary to use regularization to ensure a stable solution for this problem. Observing that TSVD is equivalent to a quadratic inequality constraint on the solution, we can achieve a similar regularization by adding a regularization term in the form of γI , where I is the identity matrix and γ is a regularization factor, to the Gramian matrix in the conjugate gradient algorithm. In this case, the solutions of both methods will be very similar.

4. RESULTS AND DISCUSSION

The results of applying the new technique to an example data set are shown in Figs. 1-2. The data used was based on manual measurement of the PSF of obtained from an ultrasound imaging data set acquired for a pin-shaped target. The proposed methods were applied to correct real data obtained from the web site of the Biomedical Ultrasound Laboratory, University of Michigan. Although the techniques proposed were applied to several data sets, the data set that was used to generate the results in this paper is the one under "Acuson17". The parameters for this data set are as follows: 128 channels, 13.8889 MSPS A/D sampling rate, 3.5 MHz transducer with 0.22mm element spacing, 2048 RF samples per line each represented in 2 bytes, and 8 averages. The data were acquired for a phantom with pins at different positions. We used the data to simulate a 48-channel beamformer on receive. The individual signals from the elements of an aperture location that coincides with one of the pins in the phantom was used for our experiments. The spatial variations

of this PSF from the location of the pin-shaped target were computed using Field II program²³. Notice the improvement of the PSF in the lateral (horizontal) direction. The improvement of the axial direction is minimal, which is expected given the larger step (in terms of number of points) used in this direction. It should be noted that the distance scales in the lateral and axial directions are different (the lateral is much larger in actual size).

It should be noted that the size and location of the large matrix elements that are selected to achieve the kernel energy percentage may be changed at will from one row to another. This means that the PSF kernel used to perform the mapping can be spatially-variant. This is a unique advantage to the new technique as compared to previous methods, which were able to only claim robustness within a range of variation around a fixed PSF. Even though the choice of this PSF here was selected based on phantom measurements of the ultrasound system, several strategies can be proposed to make a more adaptive selection of this important function. Since the implementation of the proposed system is envisioned to be in the form of a reconstruction table that relates the acquired RF samples to the output image, it is possible in principle to allow the user to select one of several base PSF forms and select a suitable pre-computed reconstruction table based on that for reconstruction. This makes this process similar to GAIN or TGC controls, which are varied by the sonographer to reach the best image quality. Another approach is to allow for an “adaptation” period at the beginning of a new scan (new patient or new organ in the same patient) whereby several images are computed using different PSF estimates and evaluated using a quality factor criterion²². Given the problems commonly associated with numerical quality functions used to describe medical images, the manual adjustment approach is expected to be a more practical approach.

The computational complexity of the proposed system can be shown to be $O(N^2)$ to obtain the solution to the linear system. This computational complexity is well within the range for conventional gridding methods as well as new gridding techniques based on SVD. The ability of the user to control the construction time is a unique feature in this iteration. This allows a quick, almost real-time computation of images for fast viewing by the sonographer. Also, it allows the sonographer to increase the accuracy of the reconstruction of a selected image at will simply by allowing additional iterations to run. Given the low complexity of iterations, such process can be performed during image viewing using console control just like zooming or gamma curve selection with virtually no noticeable delay. This is an obvious advantage of the new method.

5. CONCLUSIONS

A new strategy for ultrasound image deconvolution based on 2-D spatially-variant kernel is proposed. The new method offer a general model for the imaging process and a solution that provides an optimal reconstruction of the ultrasound image under the validity of assumptions on PSF. The proposed strategy can be utilized in tandem with previous techniques to augment axial and lateral deconvolution in one step to better model the imaging problem. Future work is needed to verify the performance of the proposed strategy under practical imaging settings.

ACKNOWLEDGEMENTS

We would like to thank Dr. Matt O'Donnell and Biomedical Ultrasonics Laboratory, University of Michigan, Ann Arbor, for making their data available to us and the ultrasound community in general. We acknowledge also the use of the Field II program by Jurgen Jensen. We acknowledge also the partial support received from International Biomedical Engineering (IBE Technologies), Giza, Egypt.

APPENDIX I: ALGORITHM FOR CONJUGATE GRADIENT ITERATION

The method of conjugate gradient describes a class of iterative techniques having the property of guaranteed convergence in a finite number of iterations^{19,20}. Also, even when the system is ill conditioned, good estimates of the largest and smallest eigenvalues are not needed to determine the algorithm parameters. The basic idea of this method is to eliminate the residual error (i.e., the difference between the right-hand and left-hand sides of the linear system equation) along directions that are all mutually orthogonal with under transformation with the system matrix and spanning the space of the solution. The original formulation of this iteration requires the system to be real, square, symmetric and positive definite for the algorithm to work and provide a unique solution to the system²⁰. Here, a

modification of the technique is applied to compute the minimal least-squares solution¹⁸. That is, it is used to solve the normal equations of the system given the properties of the Grammian matrix. In particular, the conjugate gradient algorithm for solving the normal equation $\mathbf{A}^H \mathbf{A} \vec{x} = \mathbf{A} \vec{b}$ is described as follows:

1. Set the initial solution $\vec{x}_0 = \vec{0}$.
2. Compute the initial residual $\vec{r}_0 = \vec{b} - \mathbf{A} \vec{x}_0$.
3. Compute first direction $\vec{p}_0 = \mathbf{A}^H \vec{r}_0$.
4. Compute $c_m = \|\mathbf{A}^H \vec{r}_m\|_2^2$, $d_m = \|\mathbf{A} \vec{p}_m\|_2^2$, $a_m = c_m / d_m$.
5. Update solution $\vec{x}_{m+1} = \vec{x}_m + a_m \cdot \vec{p}_m$, and update residual $\vec{r}_{m+1} = \vec{r}_m - a_m \cdot \mathbf{A} \vec{p}_m$.
6. Compute $e_m = \|\mathbf{A}^H \vec{r}_{m+1}\|_2^2 / c_m$, and update direction $\vec{p}_{m+1} = \mathbf{A}^H \vec{r}_{m+1} + e_m \cdot \vec{p}_m$.
7. Increment counter $m=m+1$, and repeat steps 4 through 6 until one of the following conditions is satisfied: $e_m = 0$, c_m is below a certain threshold, or the number of iterations reached a predetermined number N_{iter} .

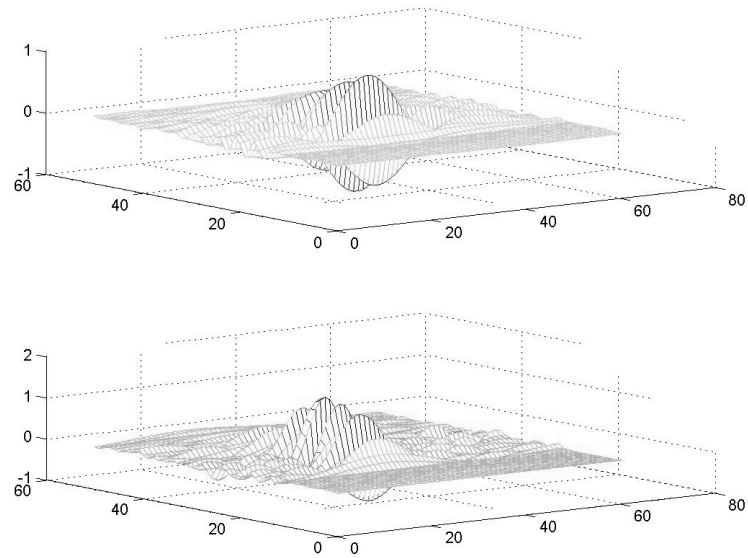


Figure 1. Surface plot for the PSF of the imaging system before (top) and after (bottom) deconvolution.

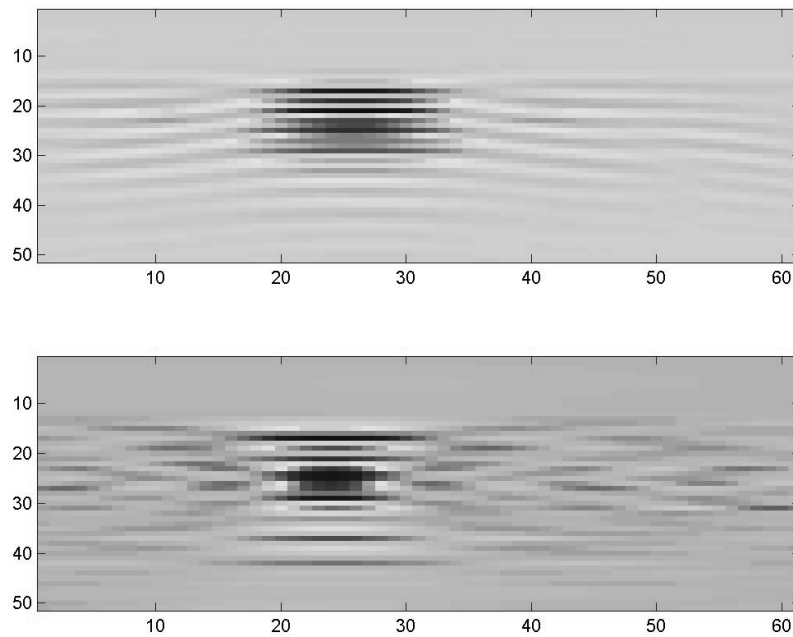


Figure 2. Image representation for the PSF of the imaging system before (top) and after (bottom) deconvolution.

REFERENCES

1. M.A. Mohamed and J. Saniie, "Improved ultrasonic B-scans using deconvolution and morphological filters," *Proc 1991 IEEE Ultrasonics Symp.*, pp. 1313-1317, 1991.
2. P.-C. Li, E. Ebbini, and M. O'Donnell, "A new filter design technique for coded excitation systems," *IEEE Trans Ultrason., Ferroelect., and Freq. Contr.* **39**, no. 6, pp. 693-699, 1992.
3. B. Haider, P.A. Lewin, and K.E. Thomenius, "Pulse elongation and deconvolution filtering for medical ultrasonic imaging," *IEEE Trans. Ultrason., Ferroelect., and Freq. Contr.* **45**, no. 1, pp. 98-113, 1998.
4. J.A. Jensen, J. Mathorne, T. Gravesen, and B. Stage, "Deconvolution of in-vivo ultrasound B-mode images," *Ultrasonic Imaging* **15**, pp. 122-133, 1993.
5. J.A. Jensen, "Estimation of in vivo pulses in medical ultrasound," *Ultrasonic Imaging* **16**, pp. 190-203, 1994.
6. T. Taxt, "Restoration of medical ultrasound images using two-dimensional homomorphic deconvolution," *IEEE Trans. Ultrason., Ferroelect., and Freq. Contr.* **42**, no. 4, pp. 543-554, 1995.
7. U.R. Abeyratne, A.P. Petropulu, J.M. Reid, T. Golas, E. Conant, and F. Forsberg, "Higher order versus second order statistics in ultrasound image deconvolution," *IEEE Trans. Ultrason., Ferroelect., and Freq. Contr.* **44**, no. 6, pp. 1409-1416, 1997.
8. X. Wang, C.J. Ritchie, and Y. Kim, "Elevation direction deconvolution in three-dimensional ultrasound imaging," *IEEE Trans. Med. Imaging* **15**, no. 3, pp. 389-394, 1996.
9. T. Olofsson and T. Stepinski, "Maximum a posteriori deconvolution of sparse ultrasonic signals using genetic optimization," *Ultrasonics* **37**, pp. 423-432, 1999.
10. W. Tobocman, D. Driscoll, N. Shokrollahi, and J.A. Izzat, "Free of speckle ultrasound images of small tissue structures," *Ultrasonics* **40**, 983-996, 2002.
11. T. Boutkedjirt and R. Reibold, "Improvement of the lateral resolution of finite-size hydrophones by deconvolution," *Ultrasonics* **38**, 745-748, 2000.
12. D. Adam and O. Michailovich, "Blind deconvolution of ultrasound sequences using nonparametric local polynomial estimates of the pulse," *IEEE Trans. Biomed. Engineering* **49**, no. 2, pp. 118-131, 2002.
13. T. Taxt, "Three-dimensional blind deconvolution of ultrasound images," *IEEE Trans. Ultrason., Ferroelect., and Freq. Contr.* **48**, no. 4, pp. 867-871, 2001.
14. T. Taxt and Jarle Strand, "Two-dimensional noise-robust blind deconvolution of ultrasound images," *IEEE Trans Ultrason., Ferroelect., and Freq. Contr.* **48**, no. 4, pp. 861-866, 1998.
15. T. Lango, T. Lie, O. Husby, and J. Hokland, "Bayesian 2-D deconvolution: effect of using spatially invariant ultrasound point spread functions," *IEEE Trans. Ultrason., Ferroelect., and Freq. Contr.* **48**, no. 1, pp. 131-141, 2001.
16. O. Husby, T. Lie, T. Lango, J. Hokland, and H. Rue, "Bayesian 2-D deconvolution: a model for diffuse ultrasound scattering," *IEEE Trans. Ultrason., Ferroelect., and Freq. Contr.* **48**, no. 1, pp. 121-130, 2001.
17. U.R. Abeyratne, A.P. Petropulu, and J.M. Reid, "Higher order spectra based deconvolution of ultrasound images," *IEEE Trans. Ultrason., Ferroelect., and Freq. Contr.* **42**, no. 6, pp. 1064-1075, 1995.
18. G. H. Golub and C. F. Van Loan, *Matrix Computations*, 2nd ed., The Johns Hopkins University Press, Baltimore, 1989.
19. M. R. Hestenes, *Conjugate Direction Methods in Optimization*, Springer-Verlag, Heidelberg, Germany 1980.
20. Y. M. Kadah and X. Hu, "Algebraic reconstruction for magnetic resonance imaging under B0 inhomogeneity," *IEEE Trans. Med. Imag.* **17**, no. 3, pp. 362-370, June 1998.
21. W. H. Press, S. A. Teukolsky, W. T. Vetterling, and B. P. Flannery, *Numerical Recipes in C: The Art of Scientific Computing*, 2nd ed., Cambridge University Press, Cambridge, 1992.
22. L. Nock and G.E. Trahey, "Phase aberration correction in medical ultrasound using speckle brightness as a quality factor," *J. Acoust. Soc. Am.* **85**, no. 5, pp. 1819-1833, 1989.
23. J.A. Jensen and N.B. Svendsen, "Calculation of pressure fields from arbitrarily shaped, apodized, and excited ultrasound transducers," *IEEE Trans. Ultrason., Ferroelec., Freq. Contr.* **39**, pp. 262-267, 1992.